JGR Earth Surface

RESEARCH ARTICLE
10.1029/2023JF007612

The Role of Talus Pile Mobility in Valley Widening Processes and the Development of Wide Bedrock Valleys, Buffalo River, AR

O. H. Groeber[1,2] and A. L. Langston[1]

[1]Department of Geography and Geospatial Sciences, Kansas State University, Manhattan, KS, USA, [2]Now at Farmington Metropolitan Planning Organization, Farmington, NM, USA

Key Points:

- Our data tests a process-based model linking bedrock valley width with how quickly river export collapsed talus away from valley walls
- In this field site, talus blocks are larger and difficult to transport in narrow valleys, while wide valleys have smaller talus blocks
- Wide bedrock valleys can develop where rivers efficiently transport talus away from valley walls; rarely transported talus can inhibit valley widening

Supporting Information:

Supporting Information may be found in the online version of this article.

Correspondence to:

A. L. Langston,
alangston@ksu.edu

Citation:

Groeber, O. H., & Langston, A. L. (2024). The role of Talus pile mobility in valley widening processes and the development of wide bedrock valleys, Buffalo River, AR. *Journal of Geophysical Research: Earth Surface*, *129*, e2023JF007612. https://doi.org/10.1029/2023JF007612

Received 5 JAN 2024
Accepted 19 JUL 2024

Author Contributions:

Conceptualization: A. L. Langston
Data curation: O. H. Groeber
Formal analysis: O. H. Groeber, A. L. Langston
Funding acquisition: A. L. Langston
Investigation: O. H. Groeber
Methodology: O. H. Groeber, A. L. Langston
Project administration: A. L. Langston
Resources: O. H. Groeber, A. L. Langston
Software: A. L. Langston
Supervision: A. L. Langston
Visualization: O. H. Groeber
Writing – original draft: O. H. Groeber, A. L. Langston

Abstract Valley width is largely controlled by lithology and upstream drainage area, but little work has focused on identifying the processes through which valleys widen. Bedrock valleys widen by first laterally eroding bedrock valley walls, followed by the collapse of overlying bedrock material that must then be transported away from the valley wall before the valley can continue widening. We hypothesize that talus piles that cannot be transported by the river protect the valley wall and slow valley widening, while talus piles that are rapidly transported allow for uninterrupted valley widening. We used field measurements from 40 locations in both wide and narrow valleys along the Buffalo River, AR to test this hypothesis. Our data show that wide valleys tend to have fewer talus piles and smaller talus grain sizes, whereas talus in narrow valleys is larger in size and more continuous along valley walls. We calculated potential talus block entrainment at each site location and found that talus blocks in wide valleys are potentially entrained and moved away from valley walls during moderate and large flood events, whereas talus blocks in narrow valleys are very rarely moved. Our results show that the potential transport of talus piles protecting bedrock valley walls from widening is controlled by the block size of collapsed bedrock wall material relative to stream competency. Our results also suggest that persistence versus mobility of collapsed talus piles is an important process in the development of wide bedrock valleys.

Plain Language Summary The width of a river valley largely depends on the rock type of the valley walls and the size of the upstream watershed, but we know very little about how a wide bedrock valley is formed. A river widens a bedrock valley by first undercutting the valley wall, causing the overlying material to collapse into the valley bottom. Then, the river must transport the collapsed material away from the valley wall so that the widening can continue. We use field data to test a conceptual model that links the width of bedrock valleys with how easily rivers can transport collapsed wall material. We measured the size of talus blocks and river channel geometry at 40 locations along the wide and narrow valleys of the Buffalo National River in northwest Arkansas. Next, we calculated whether moderate to very large floods can transport talus blocks away from valley walls. We found that in wide valleys the river can sometimes transport talus, while in narrow valleys, no talus blocks could be transported even in the 1000-year flood. Our results suggest that the widening of bedrock valleys could be stalled by large, immobile blocks of talus that shield valley walls from undercutting and eventual widening.

1. Introduction

Bedrock river valleys exhibit significant variations in width, offering valuable insights into their evolutionary history and the underlying geomorphic processes that formed them. This paper seeks to enhance our understanding of the processes governing bedrock valley widening and the crucial factors influencing the development of wide versus narrow bedrock valleys. Developing a process-based understanding of how bedrock valleys widen has important implications for improving numerical models of strath terrace formation (e.g., Langston & Tucker, 2018), the coupling of hillslopes with channels (e.g., Gabet, 2020; Sklar et al., 2017), and characterizing controls on aquatic habitat unit distribution and stability (e.g., May et al., 2013).

In the absence of significant tectonic activity, climate largely controls whether a river carves a wide or narrow bedrock valley through its influence on both sediment and water transport dynamics (e.g., Clubb et al., 2023; Schanz et al., 2018; Wegmann & Pazzaglia, 2002). Increased sediment flux relative to water discharge encourages lateral erosion and valley widening (Bufe et al., 2017; Bull, 1991; Gilbert, 1877; Hancock &

Writing – review & editing:
O. H. Groeber, A. L. Langston

Anderson, 2002; Langston & Robertson, 2023; Merritts et al., 1994), while shifts toward reduced sediment load or increased river discharge can lead to vertical valley incision (Dühnforth et al., 2012; Hanson et al., 2006). Climate influences both sediment flux and river discharge, suggesting that valley morphology can potentially serve as a proxy for past climate regimes (Meyer et al., 1995; Whittaker, 2012; Wobus et al., 2006). Strath terraces, floodplains of wide bedrock valleys that were abandoned through river incision, provide critical evidence of times when lateral erosion exceeded vertical incision, and are often (but not always (e.g., Limaye & Lamb, 2014)) associated with changes in climate (Devecchio et al., 2012; Pan et al., 2003; Vandenberghe, 2003). In order to improve interpretations of strath terraces as climate proxies, we first aim to better understand the timescales of valley widening and the processes that govern bedrock valley evolution by identifying and quantifying controls on bedrock valley width.

River discharge and bedrock lithology have been identified as primary controls on valley width following a power law relationship (Brocard & van der Beek, 2006; Langston & Temme, 2019; Tomkin et al., 2003). This relationship for valley width is given by $V_w = KA^c$ where K is bedrock erodibility, A is drainage area, and c is an exponent that ranges between 0.3 and 0.6, but is often equal to 0.4 in many places (Beeson et al., 2018; Brocard & van der Beek, 2006; May et al., 2013; Schanz & Montgomery, 2016; Snyder et al., 2003; Turowski et al., 2023). Valley width typically increases going downstream as discharge increases (Tomkin et al., 2003; Whipple, 2004; Wohl & David, 2008), and wider bedrock valleys tend to occur more often in easily erodible lithologies (e.g., weakly cemented sandstone, shale) than in more resistant lithologies (Johnson & Finnegan, 2015; Schanz & Montgomery, 2016).

While drainage area and lithology are well-established parameters explaining width differences among bedrock valleys (e.g., Brocard & van der Beek, 2006; May et al., 2013; Montgomery, 2004; Snyder et al., 2003; Tomkin et al., 2003), mechanisms that directly link discharge and lithology to bedrock widening processes remain incompletely understood. A novel conceptual model proposed two end members of bedrock valley widening to explain variations in valley width beyond the influences of drainage area and lithology (Langston & Temme, 2019). This model outlines a two-step process: first, lateral erosion and undercutting of the bedrock riverbank followed by the eventual collapse of the overlying valley wall; and second, the removal of the collapsed material from the base of the valley wall. This model proposes that the duration for which collapsed material shield valley walls from further lateral erosion is an important control on valley width.

In this study, we embark on the first field test of the conceptual model from Langston and Temme (2019) by documenting talus pile characteristics and calculating potential talus transport in the wide and narrow bedrock valleys of the Buffalo National River in Arkansas. If the model accurately represents the dynamics of valley widening, we expect to find wide valleys where the river efficiently transports collapsed talus blocks from the base of the valley wall. Conversely, in areas where the river is less effective at moving collapsed talus blocks away from valley walls, we expect persistent talus piles to shield the bedrock valley wall from further widening, ultimately leading to narrower valleys.

Our study aims to address two primary research questions that investigate the role of talus in the development of wide bedrock valleys:

1. What are the grain size distributions of talus piles found in wide and narrow bedrock valleys within the Buffalo National River?
2. What magnitude of flood event is necessary to transport the talus grain sizes in wide versus narrow bedrock valleys?

By answering these questions, we begin to explore the relationship between bedrock valley width and how frequently a river can access the bedrock wall and actively widen the valley by assessing the relative mobility or persistence of protective talus cover at the base of valley walls.

2. Field Site and Methods

2.1. Field Site Description

Our field site is located in the upper reaches of the Buffalo National River (Figure 1) in northwest Arkansas. The main stem of the river runs ~238 km from its headwaters to the confluence with the White River. The climate is humid with an average annual precipitation of ~120 cm/yr, with most precipitation occurring during the mid-

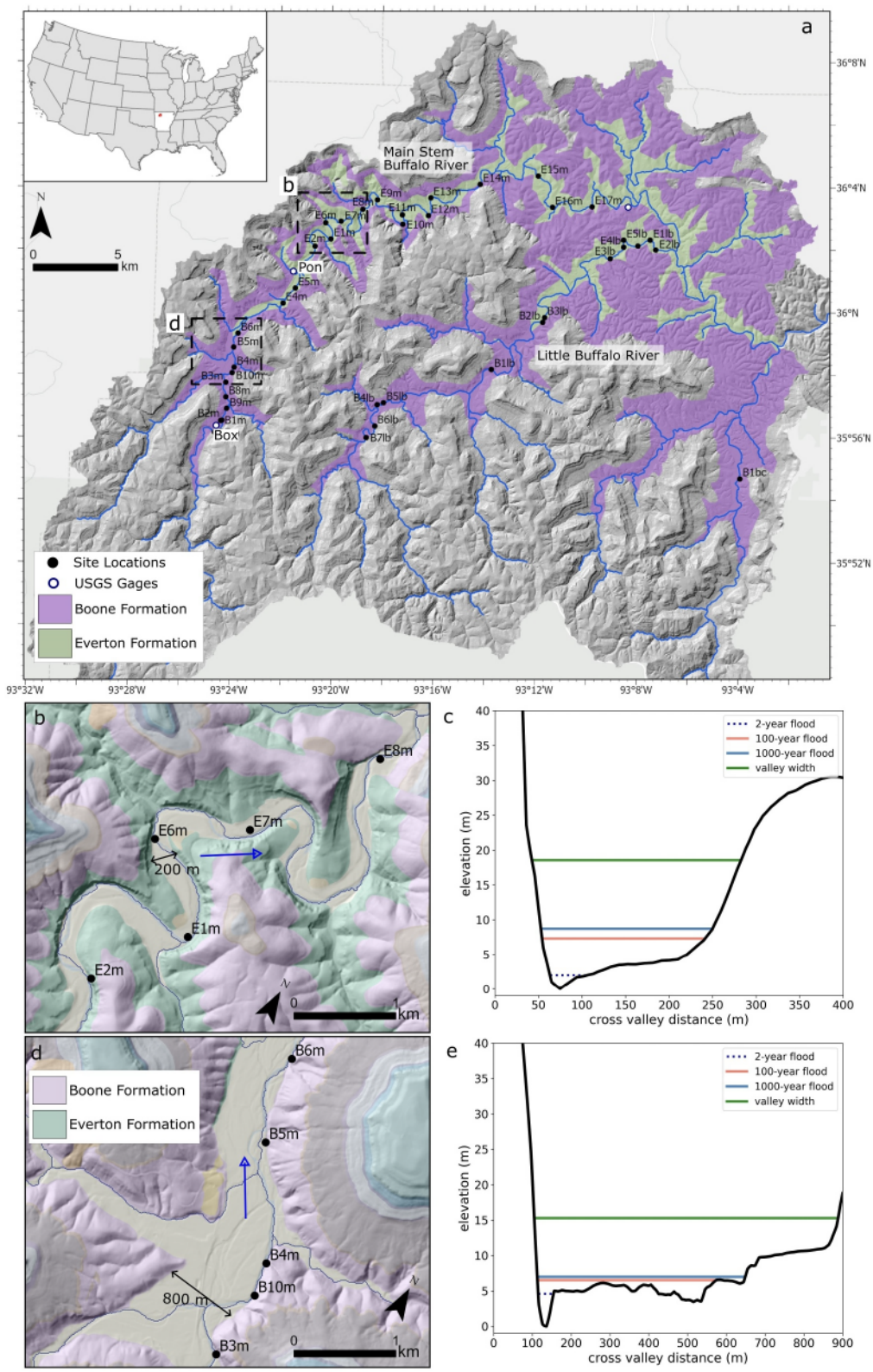

Figure 1.

spring to early summer months. The river is strongly influenced by the karst system underlying the watershed and exhibits a very flashy flow regime that responds rapidly to rain events. The USGS maintains several discharge gages along the river; we used data from two discharge stations in this study. The discharge station at Boxley (USGS station ID#07055646) has data records since 1993 and is located near our most upstream field site in the wide valley reach. The station at Ponca (USGS station ID#07055660) has discharge records dating from 2008 and is located at the beginning of the narrow valley reach (Figure 1).

Our study reaches have both wide and narrow bedrock valleys. We define a wide valley as having a valley width many times (10×) greater than the channel width and a narrow valley is one whose valley is only a few times wider than the channel width (Langston & Tucker, 2018). In our study reaches, river valleys range from 500 m to over 1,500 m wide, and the narrow valleys range from 100 to 250 m wide (Figure 1). Wide valleys occur in the upstream reaches of both the Main Stem of the Buffalo River (9 km long) and the Little Buffalo River (23.3 km), the largest tributary of the Buffalo River. Narrow valleys are found in the downstream study reaches of both rivers (Main Stem 51 km long, Little Buffalo 9 km long), although landslides can cause smaller scale valley narrowing in both wide and narrow reaches.

Valley width along the Buffalo River is controlled by local lithology (Keen-Zebert et al., 2017). The study area is dominated by two lithological units, the Mississippian-aged Boone Formation and the Ordovician-aged Everton Formation. A distinct trend in valley narrowing occurs downstream of the lithological transition between the Boone and Everton Formations (Figure 1c). The Boone Formation, found in the upstream reaches of the study area, is a medium to thick bedded chert bearing limestone that is 95–115 m thick (Hudson & Turner, 2007) and commonly contains karst features such as caves and sinkholes. The Everton Formation occurs in the downstream sections and is an interbedded sandstone, dolomite, and limestone sequence that is 95–110 m thick in the study area (Hudson & Murray, 2003). The Newton Sandstone Member of the Everton is a well sorted quartz arenite that makes up the more prominent bluffs along the Main Stem Buffalo River (Hudson & Murray, 2003; Keen-Zebert et al., 2017; Zunka, 2018). Schmidt hammer rebound values correlate with compressive rock strength and can be used to characterize rock erodibility (Aydin & Basu, 2005; Goudie, 2006; Roda-Boluda et al., 2018). Previous work in our study area has found that Schmidt hammer values are higher in the Boone Formation than in the Everton Formation (Keen-Zebert et al., 2017; Thaler & Covington, 2016). While the Schmidt hammer measurements could suggest greater resistance to physical erosion in the Boone Formation compared to the Everton, susceptibility to chemical weathering is significantly higher in the limestones of the Boone than in the dolostones of the Everton (Keen-Zebert et al., 2017). Fracture spacing can also play a role in reach-scale bedrock erodibility. We observed greater fracture spacing in sections of the Everton Formation, especially the Newton Sandstone, compared to the Boone Formation, but fracture spacing is quite variable across both formations (Hudson & Murray, 2003; Hudson & Turner, 2007).

2.1.1. Site Selection

Potential field sites were initially identified using topographic, geologic, digital elevation maps, and Google Earth. The primary selection criterion was the presence of a steep bank or bluff with exposed bedrock adjacent to the river channel. The abundance of talus was not a determining factor. The final decision for accepting a field site was made during field visits based on accessibility. Of the 26 sites on the Main Stem Buffalo River, 10 were in the Boone Formation and 16 were in the Everton Formation. Thirteen sites were located on the Little Buffalo River, with seven locations in the Boone formation and six in the Everton Formation (Figure 1).

Figure 1. (a) Upper Buffalo River watershed with site measurement locations and USGS discharge gage locations shown over a simplified geological map. Blue arrows indicate river flow direction. Wide bedrock valleys are found in the Boone Formation (pink shading) and narrow valleys are found in the Everton Formation (green shading). (b) Narrow bedrock valleys on the Main Stem Buffalo River. In this reach of the river, the dolostones and sandstones of the Everton Formation create bedrock bluffs ~75 m tall and the valley bottom is typically ~150–200 m wide. (c) Narrow valley cross-section at location E6m with measured valley width indicated with a green line and calculated widths and heights of the 2-year, 100-year, and 1000-year floods indicated by dashed, orange, and blue lines. (d) Wide bedrock valleys in the upstream reaches of the Main Stem Buffalo River. The bedrock valley walls are made up of Boone Formation limestone and range from 15–85 m above river elevation. The valley bottom is ~500–800 m wide in this reach. (e) Wide valley cross-section at location B10m with measured valley width indicated with a green line and calculated widths and heights of the 2-year, 100-year, and 1,000-year floods indicated by dashed, orange, and blue lines.

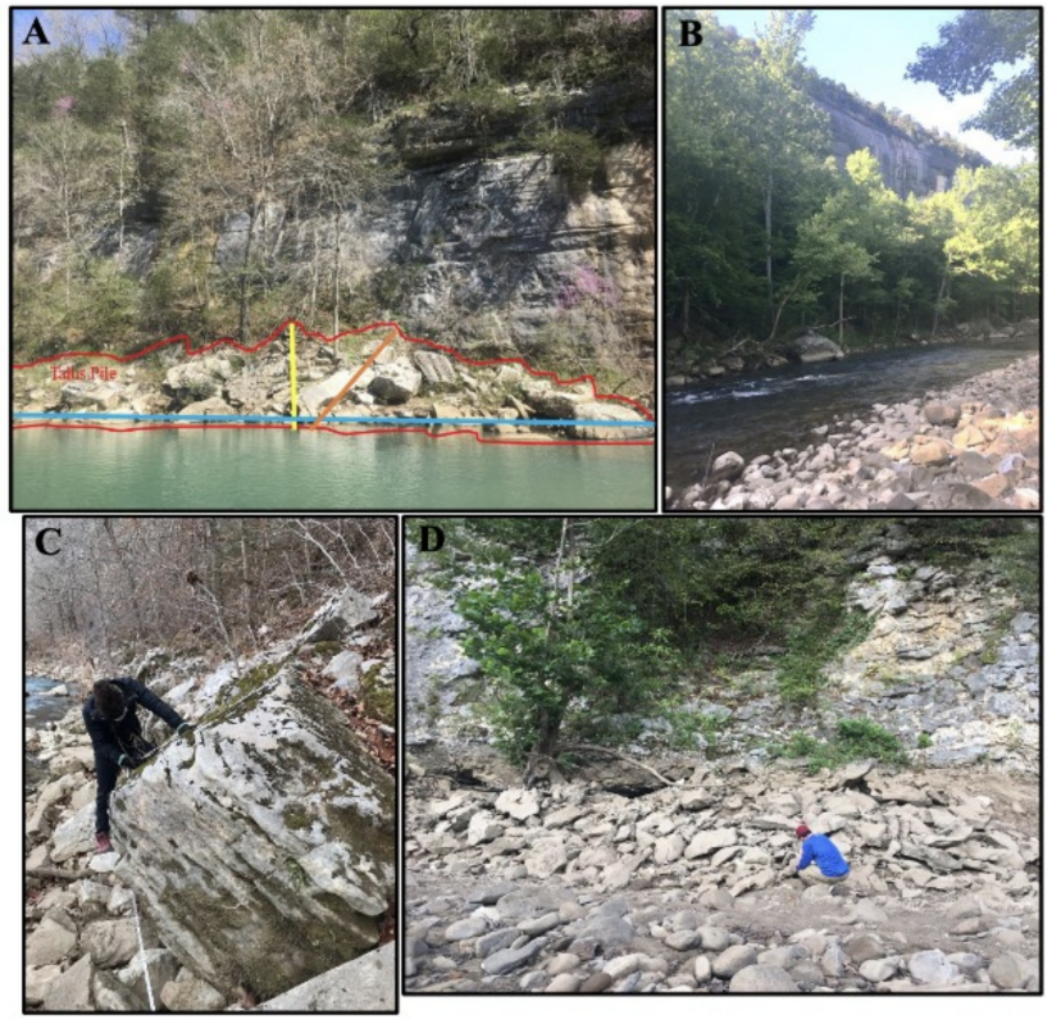

Figure 2. (a) Talus at site E4m. The D_{50} grain size of the talus at this site is 341 mm, and the D_{84} talus grain size is 627 mm. The talus pile is outlined in red, the yellow line is the vertical height of the talus pile (7 m), and the orange line indicates the depth of the pile. The blue line indicates the horizontal length of the pile (65 m), part of which extends outside the picture frame. (b) Pictured is site E11m; mature trees and woody vegetation cover much of the talus pile. The tall bedrock valley wall is visible in the background. This talus pile and the bedrock valley wall extend hundreds of meters along the river's edge. (c) Measuring large talus grains at E1m using a measuring stick on the intermediate axis. (d) Measuring talus grains at B8m using a measuring tape.

2.2. Field Measurements

At each field site, we measured grain sizes of channel and bar sediments, grain sizes of talus blocks at the base of valley walls, and bankfull width. We characterized the grain size distribution of the bedload from the riverbed and cobble bars using the Wolman pebble count method. At least 100 individual bed grains at each site were measured within the range of 5.6 mm to ≥300 mm using a standard gravel meter. Grain sizes of sediments in channels and bars reflect sediment sizes that are transported by the river with some regularity. Given that the last major flood in the study area occurred 11 years before our field measurements, we assume that the measured bed and bar sediment reflects sediment transport during typical flow conditions as opposed to flood transport.

Similarly, we characterized the grain size distribution of talus blocks in piles at the base of valley walls (Figure 2). The goal was to measure a minimum of 50 talus blocks at each site, but we often measured more than 60 individual talus blocks. If a talus pile had fewer than 50 blocks, we measured all talus blocks in the pile. We measured the intermediate (*b*-axis) of each block using a measuring stick (Verdian et al., 2020). Occasionally, we observed talus blocks in the pile that showed signs of river transport, such as rounding or imbrication; these blocks were

excluded from the talus grain size count. In order to systematically measure talus grains from different areas of the talus piles, two 30-m-long transects were established along the talus pile parallel to the valley wall, one transect along the lower section of the talus pile closest to the river and one transect in the upper section of the pile. Additionally, we placed at least two perpendicular transect lines, stretching from the waterline to the top of the talus pile or the valley wall. If the length of the talus pile was shorter than 30 m, the transects parallel to the valley wall ran across the entire length of the pile. The volume and geometry of talus piles varied among sites, leading to variable transect lengths from site to site. Individual block sizes were measured every 0.5 m unless talus blocks at a site were 1.0 m or greater in diameter, in which case we used a 1.0 m interval for measuring talus grain sizes. Statistical analysis showed no significant difference in the means between measurements taken at 0.5 m and 1 m for the same talus pile.

We used 9 m DEMs (USGS, 2023) to extract drainage area and slope information at each measurement location. Channel slope was calculated by averaging data over a 400 m span obtained from stream profiles extracted from the 9 m resolution DEM. DEM-derived drainage areas were used to calculate site-specific discharges. At each site location, we measured valley width from the 9 m DEM. Valley width was determined by measuring the distance between the bedrock valley walls or the distance between a bedrock valley wall and a break in cross-section slope between the floodplain and higher terrace surfaces on the opposite side of the valley (Figures 1b–1e).

2.3. Discharge and Shear Stress Calculations

We calculated the magnitude of the 2-year, 100-year, and 1,000-year flood discharges at each sample location using discharge records from two USGS gage stations in our study area (Boxley and Ponca) and reported 100-year and 500-year flood magnitudes at five locations in our study reach (Neely, 1985). We first plotted the reported 100-year and 500-year flood discharges reported by Neely (1985) at six locations in our study against the respective drainage areas and applied linear regression analysis to fit straight lines to these data points (Figure S1 in Supporting Information S1). These five locations are identified in Neely (1985) as Boxley, Ponca, Steel Creek, Kyle's Landing, Ozark, and Pruitt and correspond to our study sites B3m, E5m, E1m, E12m, and E17m, respectively. The R2 values for the 100-year and 500-year flood discharge versus drainage area relationship calculated from Neely (1985) were 0.997 and 0.996, respectively (Figure S1 in Supporting Information S1). We applied the same method to determine the drainage area - discharge relationship in our study area using discharge records from two USGS discharge stations in our study area (Boxley and Ponca). The linear fits for drainage area versus flood discharges from the two USGS gages and Neely (1985) had very similar slopes (2.96 and 3.07, respectively), but the magnitude of discharges reported by Neely (1985) were higher than those we calculated from the 30-year discharge record at Boxley (Figure S1 in Supporting Information S1).

After we confirmed that we could expect a robust drainage area—discharge relationship using discharge records from only the Boxley and Ponca gages (Figure S1 in Supporting Information S1), we then calculated 2-year, 100-year, and 1000-year floods for analysis in this paper. We plotted the predicted 2-year, 100-year, and 1,000-year discharges from the two discharge stations against the respective drainage area at the gage station and applied linear regression analysis to fit straight lines to these data points (Figure S1 in Supporting Information S1). The equations derived from the fitted lines enabled us to calculate discharge at each site location based on the specific drainage area of each individual measurement site (Figure S1 in Supporting Information S1).

Collapsed talus blocks are potentially transported away from valley walls by shear stress exerted by the river. We calculated shear stresses during 2-year, 100-year, and 1,000-year flood events as follows:

$$\tau_b = \rho g H_{max} S \tag{1}$$

where τ_b is the boundary shear stress, ρ is the density of water, g is gravity, H_{max} is the maximum flow depth during each flood size, and S is the slope of each site (Figure 3). We found H_{max} at each site by progressively increasing the flow depth in valley cross sections until the calculated discharge was within 1% of the discharge found from the linear regressions. We calculated discharge for each site as follows:

$$Q = \frac{w R^{\frac{5}{3}} S^{\frac{1}{2}}}{n} \tag{2}$$

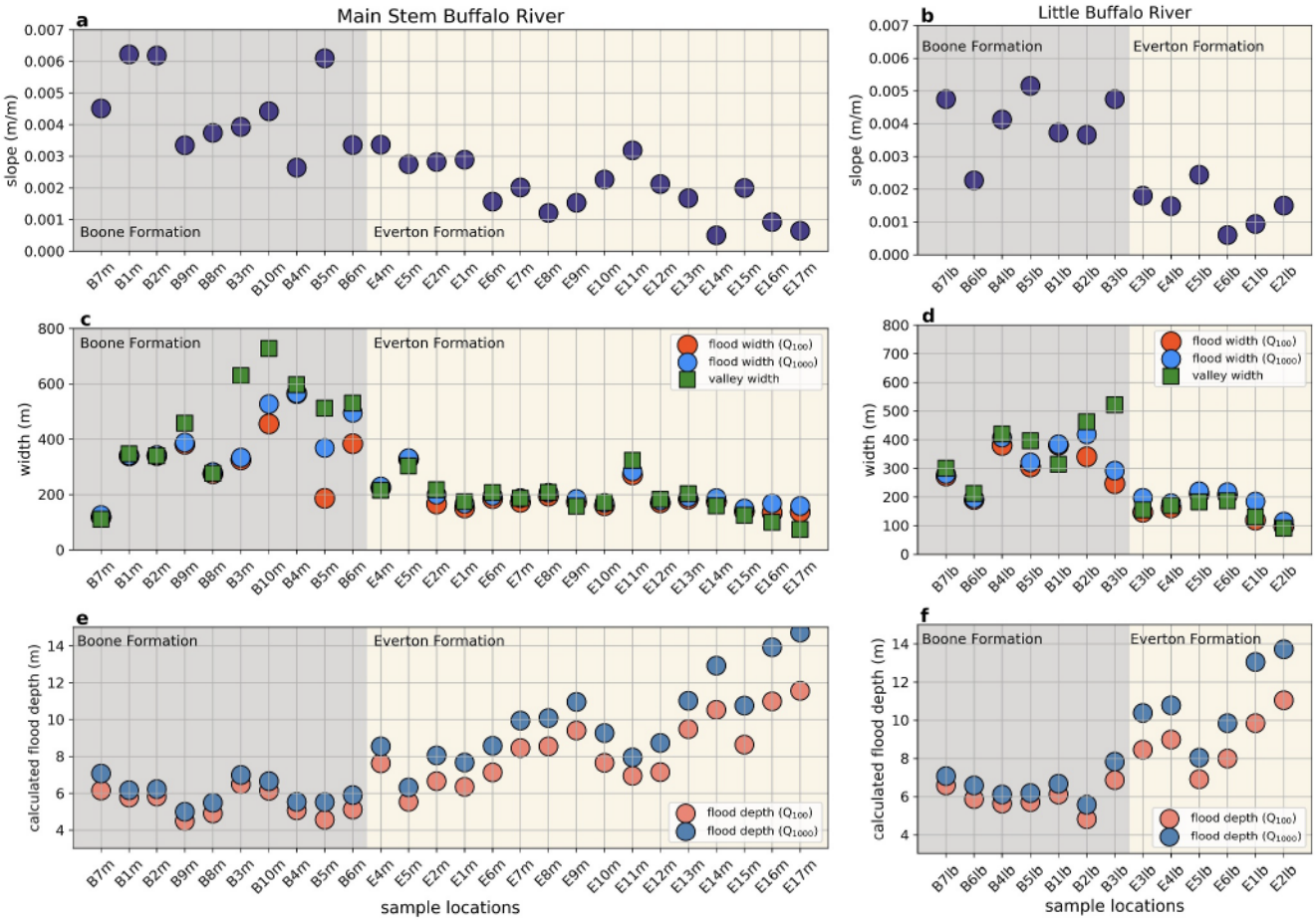

Figure 3. Slope (a, b), measured valley widths and calculated flood widths (c, d), and calculated flood depths (e, f) for the Main Stem and Little Buffalo Rivers. Where the calculated flood width is wider than the measured valley width (e.g., locations E16m, E17m), the calculated flood width covers terrace surfaces that are 10–15 m higher than the channel elevation (Figure S3 in Supporting Information S1).

where w is the calculated channel flood width, R is the hydraulic radius, and n is Manning's roughness coefficient. We used 0.04 for Manning's roughness coefficient at all sites (Neely, 1985). We then found H_{max} as the difference between the flood elevation for the calculated flood discharge and the lowest point on DEM-derived valley cross sections from each site location (Figures 1c and 1e). Our calculated 100-year flood heights agree reasonably well with documented 100-year flood heights from flooding in 1982 on the Buffalo River (Neely, 1985) (Figure S2 in Supporting Information S1).

The minimum shear stress needed to potentially move a certain grain size is determined by the critical shear stress:

$$\tau_c = \theta(\rho_s - \rho_f)gD \tag{3}$$

θ is the non-dimensional Shields parameter (with $\theta = 0.045$ in this study (Buffington & Montgomery, 1997), ρ_s is the density of rock, ρ_f is the density of water, g is acceleration due to gravity, and D is the diameter of the grain size being considered, in meters.

Entrainment of sediment grains by a river depends on the boundary shear stress imposed by the river and the size of the sediment grains. Other factors such as grain packing, grain shape, and vegetation also play a role in sediment entrainment (Yager et al., 2018; Yang et al., 2015), but these factors are not considered in our calculations. We calculated critical shear stresses of the D_{84} and D_{50} grain sizes for both bedload and talus at each of our field sites. Using calculated shear stresses at each site location during the 2-year, 100-year, and 1,000-year flood events we then determined excess shear stress for the different flood events and grain sizes, $\tau_{excess} = \frac{\tau_b}{\tau_c}$.

When excess shear stress is less than one, sediment grains are below the potential transport threshold for a particular shear stress; when excess shear stress is greater than one, sediment transport becomes possible.

3. Results

The talus piles observed throughout the study areas showed significant variation in terms of talus abundance, volume, and geometry. Some talus piles consisted of only a small number of blocks perched on exposed bedrock ledges, others formed half-cone-shaped piles of talus, while other talus piles covered the base of the bedrock valley wall for hundreds of meters (Figure 2). We observed fewer talus piles at the measurement locations in the Boone Formation reaches. Out of 40 measurement sites, six sites did not have a talus pile at the base of the valley wall; five locations with no talus pile were in the Boone Formation and one was in the Everton Formation. In the narrow valleys of the Everton Formation, the talus piles were notably more laterally extensive compared to those in the wide valleys of the Boone Formation, and often extended along the valley wall for several hundred meters.

3.1. Bedload and Talus Grain Size Distributions

Bedload grain size generally decreased as expected going downstream in our study reaches with the D_{50} bedload ranging from 26 to 140 mm (Figure 4), but we found significant and substantial differences in talus grain size between the wide and narrow valley study reaches. On the Main Stem Buffalo River, the talus blocks of the Boone Formation were significantly ($p = 1e{-}5$; Figure S4 in Supporting Information S1) and substantially smaller than talus in the Everton Formation, although the largest talus blocks were similar in size in the Boone (1,021 mm) and Everton (1,080 mm). Although talus was generally smaller in the Boone Formation, there was a larger range in D_{50} talus grain sizes in the Boone study reaches compared to the Everton reaches. In the Boone study reaches, D_{50} talus sizes ranged from 97–600 mm, compared to D_{50} talus size range of 263–542 mm in the Everton (Figure 4; Figure S4 in Supporting Information S1). On the Little Buffalo, talus grain sizes in the Boone reach were slightly smaller overall compared to the Everton reach ($p = 0.0075$; Figure 4; Figure S4 in Supporting Information S1), but talus blocks from both reaches had a similar range in size. The limited differences in talus characteristics between the Boone and Everton sites may be due to the lack of talus data in the Boone reach of the Little Buffalo (three Boone Formation sites vs. six Everton Formation sites).

Overlap between talus and bedload grain sizes may indicate a river's ability to transport talus grain sizes during flood events. Such overlap may hint that talus piles at these locations are less persistent over time. Our results show that talus and bedload grain sizes overlap at approximately half of the site locations in the Boone Formation along the Main Stem, whereas no sites in the Everton Formation show such overlap (Figure 4). Site B7m exhibits the most overlap in terms of absolute magnitude, with the D_{84} bedload grain size 85 mm larger than the D_{16} talus grain size. Conversely, at most sites in the Everton Formation, the D_{16} talus size was on the order of 100 mm larger than the D_{84} bedload size.

There were no locations along the Little Buffalo River where the D_{84} bedload and the D_{16} talus grains overlapped, but talus and bedload grain sizes were closer in the Boone reach than in the Everton reach. In the Boone reach of the Little Buffalo, talus and bedload grain sizes were typically within 50 mm of each other, compared to the Everton reach, where the D_{16} talus was at least 80 mm larger than the D_{84} bedload grain size (site E1lb; Figure 4).

3.2. Discharge, Shear Stress, and Transport Potential

Maximum shear stress exerted by the river during 2-year, 100-year, and 1,000-year flood events generally decreased going downstream due to decreasing channel slopes (Figures 3a and 3b; Figure 5a; Figure 6a). The downstream pattern of shear stresses was also affected by flood widths. Flood widths for the 100- and 1,000-year floods follow trends in valley width: valley width increases from ~100 m up to more than 700 m going downstream within the Boone Formation before narrowing abruptly in the Everton Formation (Figures 3c and 3d). Valley width does not increase going downstream in the Everton but rather remains consistently between 150–200 m. Maximum flood depths increase going downstream, particularly in the Everton Formation reach (Figures 1c and 1d; Figures 3e and 3f), due to decreasing slope and unchanging valley width.

We assessed the potential movement of D_{50} and D_{84} grain sizes for both talus and bedload during the three flood magnitudes using excess shear stress values. During the 2-year flood, excess shear stress for the D_{50} bedload consistently exceeded the transport threshold at nearly every site location (39 out of 40) (Figure 5b; Figure 6b).

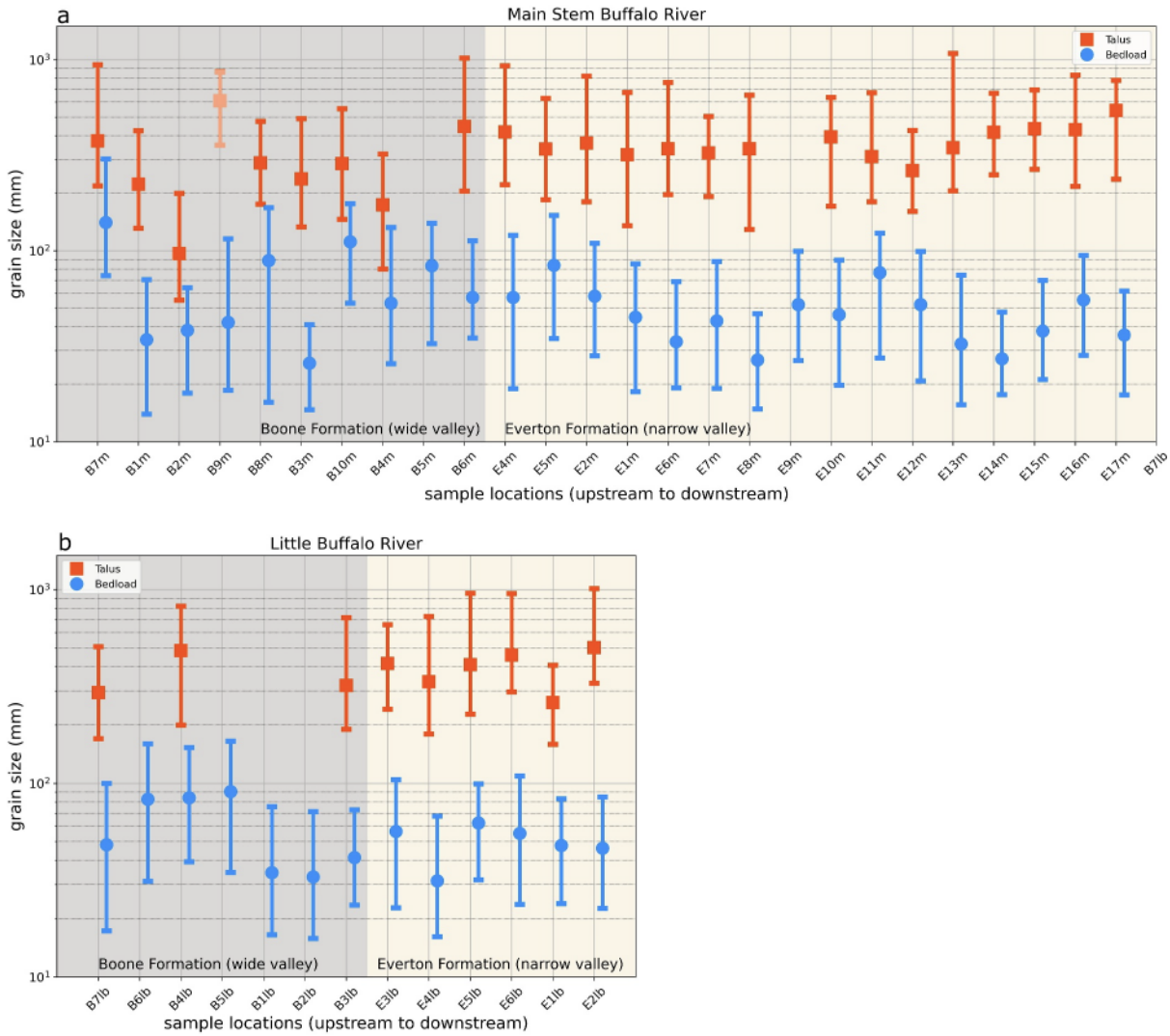

Figure 4. Talus (red) and bedload (blue) grain sizes at all site locations on the Main Stem Buffalo River (a) and the Little Buffalo River (b). The top whisker represents the D_{84} grain size, the center marker represents the D_{50} grain size, and the bottom whisker represents the D_{16} grain size. In the upstream reaches, the Boone Formation is shaded with gray boxes, and in the downstream reaches, the Everton Formation is shaded with tan boxes. (a) Main Stem Buffalo River: Site B9m is colored light orange because there are only six individual talus blocks in the distribution. We exclude B9m for the rest of our analysis. (b) Little Buffalo River: 4/7 site locations in the Boone Formation reach of the Little Buffalo had no talus pile present.

Excess shear stress for the D_{84} bedload grain size also exceeded the transport threshold at most site locations (29 out of 40) during the 2-year flood, although there was a downstream decline in the potential transport of D_{84} bedload grain sizes (Figure 5b; Figure 6b). The calculated excess shear stress values for the 2-year flood align with prior studies indicating that most bedload should be transported during such events (MacKenzie & Eaton, 2017). For both the 100-year and 1,000-year floods, excess shear stresses for the D_{50} and D_{84} bedload grain sizes were well above the transport threshold at every site (Figures S5 and S6 in Supporting Information S1).

Calculated excess shear stresses for talus grains were significantly lower than bedload grains due to the larger grain sizes of talus. During the 2-year flood event, calculated excess shear stresses for D_{50} and D_{84} talus grain sizes were well below the transport threshold at the majority of sites along both the Main Stem Buffalo River and the Little Buffalo River (Figures 7a and 8a). For the 100-year flood event, the D_{50} excess shear stress values exceeded the transport threshold at half of the sites in the Boone Formation reaches, while in the Everton Formation, the transport threshold for D_{50} talus grains was not exceeded at any of 22 sites (Figures 7b and 8b). Excess shear stresses for D_{84} talus grain sizes in the 100-year flood were below the transport threshold at nearly all sites in the Boone and the Everton.

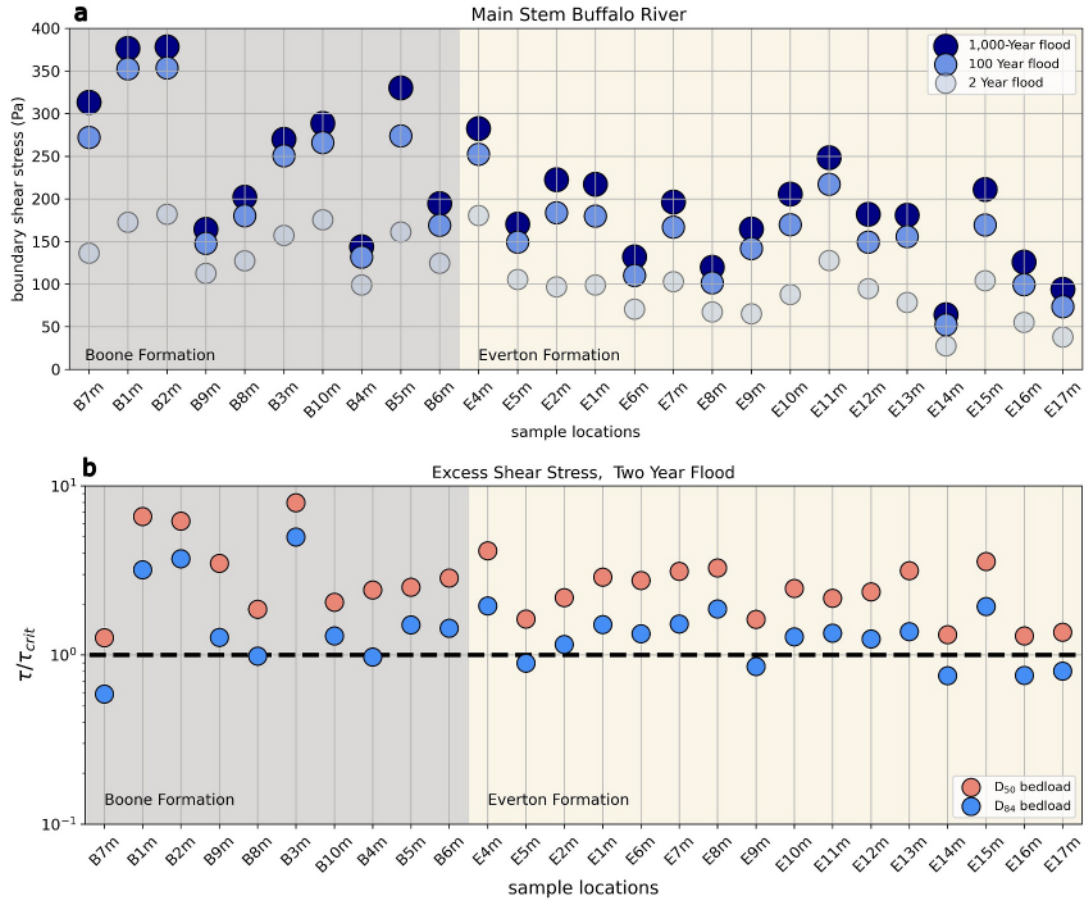

Figure 5. (a) Calculated boundary shear stress for Main Stem Buffalo River site locations for the two-year, 100-year, and 1,000-year flood discharges (Equation 2). (b) Excess shear stress (τ_b/τ_c) for the bedload material (D_{50} and D_{84}) during the calculated 2-year flood in the Main Stem Buffalo River. In the upstream reaches, the Boone Formation is shaded with gray boxes, and in the downstream reaches, the Everton Formation is shaded with tan boxes.

In the Boone Formation reaches, excess shear stress calculations for the 1,000-year flood showed little change in transport potential compared with the 100-year flood. Wider valleys in the Boone reaches allow flood waters to spread out over the valley bottom, resulting in smaller increases in flood height (Figure 3). In the Boone reaches D_{50} talus grains were potentially transportable at most (8 out of 12) sites, but even during the 1000-year flood, D_{84} grain sizes were transportable at only two sites (Figures 7c and 8c). In the Everton reaches, excess shear stress exceeds the transport threshold for the D_{50}a talus grain size at a single site (out of 22), and D_{84} talus grain sizes remain well below the threshold at every site in the Everton reaches (Figures 7c and 8c).

4. Discussion

Previous research has recognized bedrock erodibility as a pivotal factor in determining valley width, with wider valleys generally found in areas with weaker bedrock and narrower valleys in locations with more resistant bedrock (Bursztyn et al., 2015; Johnson & Finnegan, 2015; Scott & Wohl, 2019; Spotila et al., 2015; Wohl, 2008). Lithology clearly controls valley width in our study area (Figure 1) (Keen-Zebert et al., 2017), but the mechanism through which lithology creates wide versus narrow valleys is unknown.

In order to determine if the duration that the talus protects the valley wall helps determine bedrock valley width, we would ideally work in a setting where the bedrock erodibility is the same in wide and narrow bedrock valleys. Earlier research in our study area showed that Schmidt hammer values of the Boone Formation were higher than those of the Everton Formation (Keen-Zebert et al., 2017; Thaler & Covington, 2016). This could suggest greater erosional resistance in the wide valley lithology and less erosional resistance in the narrow valley lithology,

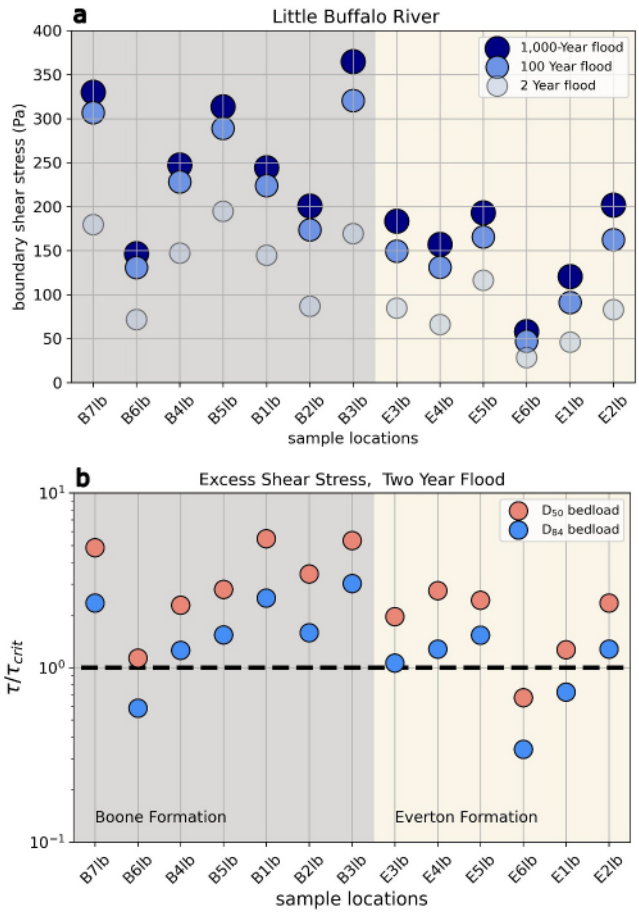

Figure 6. (a) Calculated boundary shear stress for Little Buffalo River site locations for the two-year, 100-year, and 1,000-year flood discharges (Equation 2). (b) Excess shear stress (τ_b/τ_c) for the bedload material (D_{50} and D_{84}) during the calculated 2-year flood in the Little Buffalo River. In the upstream reaches, the Boone Formation is shaded with gray boxes, and in the downstream reaches, the Everton Formation is shaded with tan boxes.

contrary to expectations based on well-established observations that wider valleys typically occur in more erodible lithology. However, bedrock erodibility is a notoriously difficult parameter to characterize (Korup, 2008; Larimer et al., 2022; Roda-Boluda et al., 2018) and centimeter-scale erodibility characterized by Schmidt hammer measurements does not encompass other rock properties that determine bedrock erodibility.

Reach scale bedrock erodibility is governed in part by fracture spacing; closer fracture spacing allows for more frequent bedrock incision through plucking and potentially less steep channel slopes (Chatanantavet & Parker, 2009; Chilton & Spotila, 2022). Denser fracture spacing in some sections of the Boone Formation compared to the Everton Formation (Hudson & Murray, 2003; Hudson & Turner, 2007) potentially results in faster rates of lateral bedrock erosion on the valley wall through plucking. Additionally, bedrock erodibility is influenced by the degree of chemical weathering. Lithologies that are more susceptible to chemical weathering (such as the limestones of the Boone Formation compared to the dolostones and sandstones of the Everton Formation) can be weakened in situ, potentially accelerating lateral bedrock erosion through dissolution (e.g., Goodfellow et al., 2016; Murphy et al., 2016).

The relief of bedrock valley walls is another way that valley-scale bedrock erodibility can potentially be assessed (Montgomery, 2001; Schmidt & Montgomery, 1995). We did not observe systematically lower relief walls in the wide valleys of the Boone and higher relief walls in the narrow valleys of the Everton (Figures 1c and 1e), although the tallest walls were in the narrow valley reach (Langston et al., 2024). This leaves open the possibility that the erodibility of the two lithological units is more similar than the fracture spacing or chemical susceptibility would suggest. We cannot disregard the possibility that the differences in valley width in our field area could be the result of different bedrock erodibilities and different rates of lateral bedrock erosion, with no significant effect of how often talus piles are transported away from valley walls. But, the similarity of metrics that characterize erodibility on both centimeter and valley scales suggests that additional mechanistic controls on valley width could also be at work.

4.1. Variation in Talus Grain Sizes

Our observations of variation in talus grain sizes between the narrow and wide valleys along the Buffalo River may shed light on the mechanisms of valley widening along the river's course. Our results show that the grain sizes of blocks in talus piles in wide valleys versus narrow valleys may be a significant factor that controls the potential transport of talus piles away from bedrock valley walls. The varying talus grain sizes may explain why narrow valleys remain narrow; larger blocks persist along the valley walls for extended periods, preventing lateral erosion at the base of the valley wall until the talus pile is eventually removed.

One possible explanation for these differences in valley width within lithological river reaches could be attributed to varying rates of chemical or physical weathering of the bedrock talus blocks. Weathering processes gradually reduce the size of talus blocks over time until they reach a size that can be transported by the river. Notably, limestone blocks of the Boone Formation tend to undergo chemical weathering at a faster rate than the sandstone and dolostone blocks of the Everton Formation (Covington et al., 2015; Covington & Vaughn, 2019; Keen-Zebert et al., 2017). In a scenario where talus blocks in wide and narrow valleys arrive at the valley bottom with similar grain size distributions but with different chemical weathering rates, the more soluble talus blocks could weather into a transportable size more rapidly. This would result in less time spent obstructing the valley wall from further lateral erosion and undercutting, potentially leading to a wider valley.

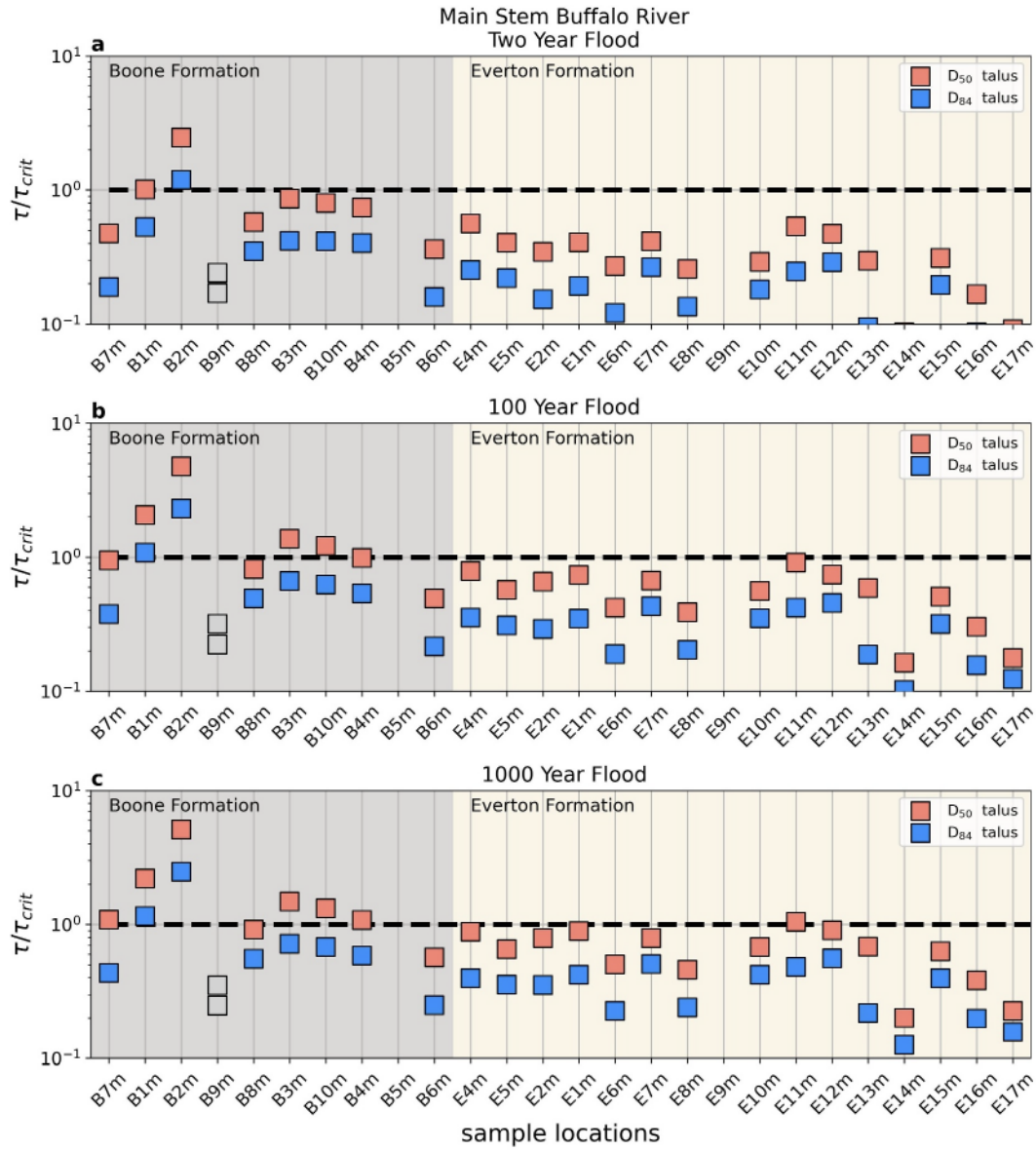

Figure 7. Excess shear stress (τ_b/τ_c) for talus grains (D_{50} and D_{84}) in the Main Stem Buffalo River during the calculated 2-year flood (a), the 100-year flood (b), and the 1,000-year flood (c). The transport threshold where excess shear stress = 1 is indicated with a black dashed line. In the upstream reaches, the Boone Formation is shaded with gray boxes, and in the downstream reaches, the Everton Formation is shaded with tan boxes. As there were only six individual talus grains at site B9m, this site was excluded from analysis.

Another plausible explanation is that talus from different lithologies arrives at the base of bedrock cliffs with substantially different grain size distributions (e.g., Attal & Lavé, 2006). Characteristics of the bedrock lithology, such as fracture spacing, affect the size of talus blocks sourced from the valley walls (Verdian et al., 2020) much as fracture spacing controls the size of blocks released by hillslopes (DiBiase et al., 2018; Sklar et al., 2017). If talus blocks arrive at the valley bottom with inherently different grain size distributions, the rate of talus block weathering does not play a critical role in determining the persistence or mobility of the talus. The smaller talus blocks should be transported away from valley walls more rapidly than larger talus blocks regardless of weathering rate.

In our study area of the Buffalo River, it appears likely that both differences in weathering rates and bedrock properties influence the grain size distributions of talus blocks, although neither of these scenarios have been

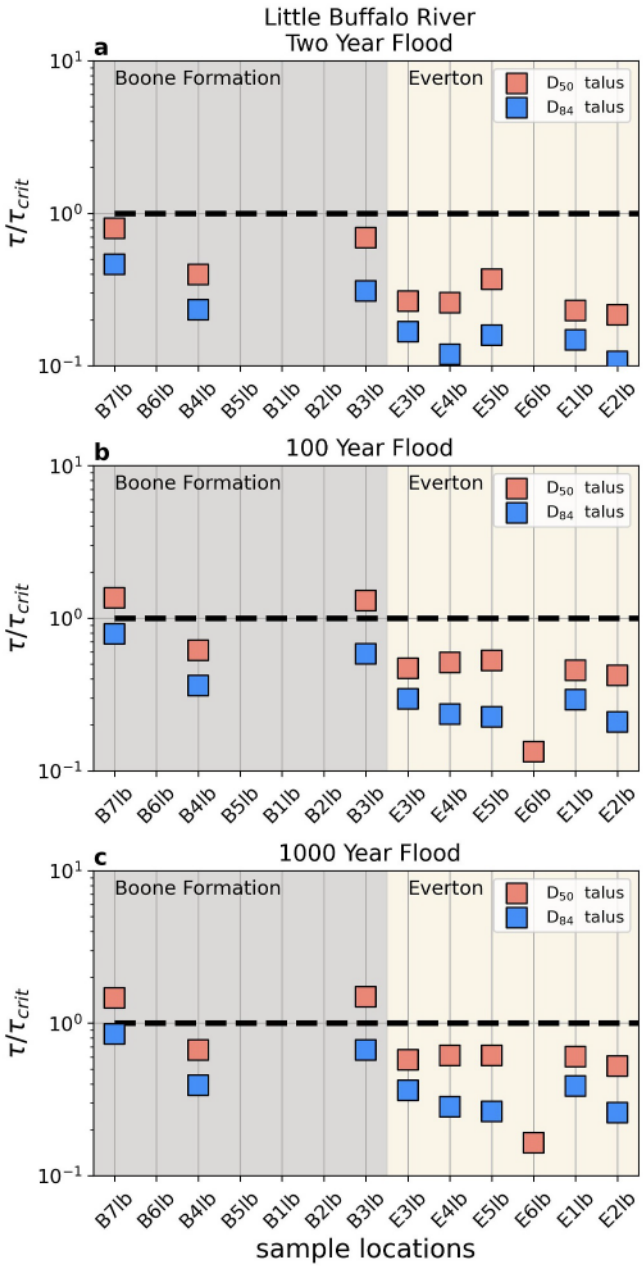

Figure 8. Excess shear stress (τ_b/τ_c) for talus grains (D_{50} and D_{84}) in the Little Buffalo River during the calculated 2-year flood (a), the 100-year flood (b), and the 1,000-year flood (c). The transport threshold where excess shear stress = 1 is indicated with a black dashed line. In the upstream reaches, the Boone Formation is shaded with gray boxes, and in the downstream reaches, the Everton Formation is shaded with tan boxes.

tested. The smaller overall talus grain size in the Boone Formation sites suggests that bedrock properties (e.g., fracture spacing) may cause talus blocks to reach the base of the valley already smaller than those in the Everton talus. The substantially larger range of talus grain sizes in the Boone Formation implies that talus piles may have a range of residence times in the valley bottom, and a range of durations of chemical weathering that reduces block size. Regardless of the primary control on talus block size in the Everton Formation, it appears that these conditions remain consistent going downstream in the river, as indicated by the remarkably uniform talus grain size distributions over a 30-km stretch and between the two study reaches (Figure 4). The vast majority of Everton talus blocks consist of sandstones and dolostones, suggesting that the chemical and physical weathering processes responsible for reducing block size occur at a much slower pace than the limestone of the Boone Formation. If talus blocks in the Everton Formation reaches were rapidly decreasing in size over time, we would expect to find a wide range of talus grain sizes along the study reach, representing talus in various stages of the weathering process.

4.2. Excess Shear Stress

We calculated maximum shear stresses acting on the riverbed to estimate the excess shear stress required to initiate the transport of talus blocks. Because flow velocity at the edges of the channel is often slowed by the presence of vegetation and other roughness elements (Yager et al., 2018; Yang et al., 2015), the actual shear stresses needed to initiate the transport of talus blocks are likely higher than our calculations indicate. Although our calculations probably underestimate shear stress, the comparison of excess shear stresses in the Boone Formation and the Everton Formation is still reasonable, as shear stress along the entire study reach is equally underestimated.

The downstream trend in excess shear stresses for talus grains is striking. Talus blocks in the Boone Formation are consistently well above the transport threshold during larger floods, whereas they abruptly fall below this threshold in the Everton Formation (Figures 7 and 8). Talus block transport is possible at half of the sites in the Boone Formation reaches during the 100-year flood, while in the Everton reaches the vast majority of talus blocks are below the transport threshold even during the 1,000-year flood. This trend lends further support to our hypothesis that the frequency of talus material transport may play a crucial role in controlling valley width: if the talus piles that line bedrock valley walls cannot be transported or are transported away from the wall very infrequently, the bedrock valley wall cannot be accessed to laterally erode and further widen the valley.

This pattern of more frequent transport of collapsed bedrock wall material in the wide valley study reaches might also explain the absence of talus piles at numerous locations in the Boone Formation, especially within the Little Buffalo River. In the Little Buffalo talus piles at the base of valley walls were present at only three out of seven sites in the Boone and when talus piles were present, they tended to have larger grain sizes than in the Main Stem (Figure 4b). The scarcity of smaller talus grains and talus piles in the Boone Formation reach of the Little Buffalo could imply that these smaller talus grains and entire talus piles are frequently transported away by the river.

Conversely, our results suggest that the talus remains in place for long intervals of time in the Everton Formation, shielding valley walls from lateral erosion and further widening. Talus blocks that are not transported by the 1,000-year flood remain in place until they weather down to a transportable size or until an extreme flood event exceeding the magnitude of the 1,000-year flood occurs to mobilize the talus blocks. Considering the relative

resistance to weathering of sandstone and dolostone talus blocks in the Everton Formation, it is likely that individual talus piles may endure substantial periods at the base of valley walls in these reaches. Moreover, if talus piles are indeed more persistent in the Everton Formation, there is a greater likelihood of vegetation being established on these piles. Although this study did not include a systematic evaluation of vegetation, there appeared to be a higher density of vegetation on the talus piles of the Everton Formation. Vegetation can both anchor the talus pile and increase bed roughness, slowing the flow and making talus block transport less likely (Yager & Schmeeckle, 2013). To initiate talus transport on vegetated talus piles, there is an additional obstacle of also exceeding the critical shear stress required to initially strip the vegetation from the talus pile.

Our results showing that D_{84} bedload grains are either above or just under the transport threshold during the two year flood (Figure 6) support the observation that bedload grain sizes observed on gravel bars typically represent grains regularly transported by the river during bankfull flows and moderate flood stage discharges (Attal et al., 2015; MacKenzie et al., 2018; Parker, 1978; Wilcock & McArdell, 1993). Consequently, a metric for describing the relationship between bedload grain size and talus grain size could be used to evaluate the potential transport of talus blocks solely from the comparison of talus and bedload grain sizes (Figure 4). The pattern of more potential talus transport in the Boone Formation reaches (Figure 7) is caused by a combination of smaller talus grain sizes and higher boundary shear stresses upstream and larger talus sizes and decreasing shear stresses downstream. The observed trend in the overlap of talus and bedload grain sizes (Figure 4) shows a similar pattern, but without the need for explicit shear stress calculations. The magnitude of grain size overlap between the talus and bedload grains appears to be related to the how close or far talus grains are from potential transport (Figures 3 and 7). At locations where the largest bedload grains and the smallest talus grains are close in size or even overlapping, talus blocks are closer to potential transport by the river, as shown by locations B7m, B2m, B10m, and E11m (Figures 3 and 7). However, where the smallest talus blocks (D_{16}) are multiple grain size classes larger than the largest (D_{84}) bedload, talus block transport is very unlikely at typical or even historic discharge levels (e.g., locations E8m, E14m, and E17m). We have not precisely defined how to quantify "overlap" between the talus and bedload grain size distributions, and such a definition is beyond the scope of this study. Despite the uncertainties of how to quantify such a transport metric from talus and bedload grain sizes, the possibility of a metric that characterizes potential transport without requiring a record of hydrological measurements is intriguing.

4.3. Implications for Channel, Valley, and Landscape Evolution

Although we cannot definitively differentiate the effects of bedrock lithology and mobility versus persistence of talus on bedrock valley width, our data support the idea that talus mobility plays a role in determining bedrock valley width and the rate of bedrock valley widening. A similar mechanism has been noted in alluvial rivers, where collapsed valley walls can shield the valley wall from further erosion (Malatesta et al., 2017). Additionally in alluvial rivers, valley wall height has been shown to limit valley width by supplying pulses of sediment that overwhelm the channel's ability to transport that sediment, and potentially force the channel to narrow (Malatesta et al., 2017; Tofelde et al., 2022). In bedrock valleys, the relationship between valley width and valley wall height has not yet been demonstrated, although it has been suggested (Langston & Temme, 2019). If valley wall height is a proxy for talus pile volume, then all else being equal, larger talus piles will take longer to evacuate, shielding valley walls for longer durations. Our results show the variability in potential talus transport and imply that the volume of the talus pile may control valley width, but only if the talus grains can be transported by the channel.

Boulders can inhibit vertical bedrock incision by shielding the channel bed and reducing flow velocity (Shobe et al., 2021), much as we conceptualize talus protecting valley walls from lateral bedrock incision. Inputs of large talus blocks can act as boulders and steepen channel slopes, creating local knickzones (Brocard & van der Beek, 2006; Thaler & Covington, 2016), can potentially narrow the channel or push it away from the valley wall and ignite a new meander, although we did not observe any of these events in our field sites. How boulder or talus armoring of the channel bed and valley wall would impact the relative rates of vertical and lateral erosion is strongly dependent on the specific fluvial setting. In a case where the channel narrows and straightens due to boulder/talus input to the channel bed, potential lateral erosion may decrease due to decreased channel curvature and laterally directed shear stress (Langston & Tucker, 2018). Alternatively, a narrowed, straightened channel may drastically increase the transport capacity of the river, allowing more rapid talus export and faster exposure of bedrock valley walls to laterally widen (Croissant et al., 2017).

5. Conclusions

Our study investigated the impact of the frequency of talus block transport on the development of wide versus narrow bedrock valleys. We collected data from 40 field locations in the Buffalo River watershed in both wide and narrow valleys. Our findings highlight significant differences in talus pile characteristics between wide and narrow valleys, with smaller and more variable talus grain sizes in wide valleys compared to larger talus blocks with little size variation in narrow valleys. Furthermore, we observed that the largest bedload grain sizes and smallest talus grain sizes often overlap in wide valleys, contrasting with the absence of overlap in narrow valleys. Excess shear stress calculations demonstrated that talus in the wide valleys is transported more frequently compared with talus in narrow valleys.

Our results suggest that the duration for which a talus pile shields the base of a bedrock valley wall may play a role in the development of wide valleys and the maintenance of narrow valleys. The size of talus blocks is only one of several factors that influence how long talus piles protect valley walls from further widening; other considerations include talus pile volume, weathering characteristics of talus blocks, and bed shear stress at the talus pile location. This study not only provides empirical support for a conceptual model of valley widening (Langston & Temme, 2019) but also advances our understanding of bedrock valley widening processes, moving beyond the classic, purely empirical approach for predicting valley width. Although these findings apply specifically to the Buffalo River, they offer a gateway for further investigation and enhanced understanding of bedrock valley widening processes.

Data Availability Statement

Field data from the Buffalo River and Little Buffalo River reported in this manuscript can be accessed at (Langston et al., 2024) https://doi.org/10.5281/zenodo.10463303.

Acknowledgments
The authors state that they have no real or perceived financial conflicts of interest. We would like to acknowledge funding from NSF grant EAR-2051559, NSF grant OIA-1833025, and the Department of Geography and Geospatial Sciences, Kansas State University. We thank Clay Robertson for his field assistance and Jill Marshall for thoughtful conversations on this manuscript.

References

Attal, M., & Lavé, J. (2006). Changes of bedload characteristics along the Marsyandi River (central Nepal): Implications for understanding hillslope sediment supply, sediment load evolution along fluvial networks, and denudation in active orogenic belts. *Special Papers - Geological Society of America*, *398*(09), 143–171. https://doi.org/10.1130/2006.2398(09)

Attal, M., Mudd, S. M., Hurst, M. D., Weinman, B., Yoo, K., & Naylor, M. (2015). Impact of change in erosion rate and landscape steepness on hillslope and fluvial sediments grain size in the Feather River basin (Sierra Nevada, California). *Earth Surface Dynamics*, *3*(1), 201–222. https://doi.org/10.5194/esurf-3-201-2015

Aydin, A., & Basu, A. (2005). The Schmidt hammer in rock material characterization. *Engineering Geology*, *81*(1), 1–14. https://doi.org/10.1016/j.enggeo.2005.06.006

Beeson, H. W., Flitcroft, R. L., Fonstad, M. A., & Roering, J. J. (2018). Deep-seated landslides drive variability in Valley width and increase connectivity of Salmon habitat in the Oregon coast range. *Journal of the American Water Resources Association*, *54*(6), 1325–1340. https://doi.org/10.1111/1752-1688.12693

Brocard, G. Y., & van der Beek, P. A. (2006). Influence of incision rate, rock strength, and bedload supply on bedrock river gradients and valley-flat widths: Field-based evidence and calibrations from western Alpine rivers (southeast France). *Geological Society of America Special Paper*, *398*, 101–126. https://doi.org/10.1130/2006.2398(07

Bufe, A., Burbank, D. W., Liu, L., Bookhagen, B., Qin, J., Chen, J., et al. (2017). Variations of lateral bedrock erosion rates control planation of uplifting folds in the Foreland of the Tian Shan, NW China. *Journal of Geophysical Research: Earth Surface*, *122*(12), 2431–2467. https://doi.org/10.1002/2016JF004099

Buffington, J. M., & Montgomery, D. R. (1997). A systematic analysis of eight decades of incipient motion studies, with special reference to gravel-bedded rivers. *Water Resources Research*, *33*(8), 1993–2029. https://doi.org/10.1029/96WR03190

Bull, W. B. (1991). *Geomorphic response to climate change* (p. 326). Oxford University Press.

Bursztyn, N., Pederson, J. L., Tressler, C., Mackley, R. D., & Mitchell, K. J. (2015). Rock strength along a fluvial transect of the Colorado Plateau - Quantifying a fundamental control on geomorphology. *Earth and Planetary Science Letters*, *429*, 90–100. https://doi.org/10.1016/j.epsl.2015.07.042

Chatanantavet, P., & Parker, G. (2009). Physically based modeling of bedrock incision by abrasion, plucking, and macroabrasion. *Journal of Geophysical Research*, *114*(4), 1–22. https://doi.org/10.1029/2008JF001044

Chilton, K. D., & Spotila, J. A. (2022). Uncovering the controls on fluvial bedrock erodibility and knickpoint expression: A high-resolution comparison of bedrock properties between knickpoints and non-knickpoint reaches. *Journal of Geophysical Research: Earth Surface*, *127*(3), e2021JF006511. https://doi.org/10.1029/2021JF006511

Clubb, F. J., Mudd, S. M., Schildgen, T. F., van der Beek, P. A., Devrani, R., & Sinclair, H. D. (2023). Himalayan valley-floor widths controlled by tectonically driven exhumation. *Nature Geoscience*, *16*(8), 739–746. https://doi.org/10.1038/s41561-023-01238-8

Covington, M. D., Gulley, J. D., & Gabrovšek, F. (2015). Natural variations in calcite dissolution rates in streams: Controls, implications, and open questions. *Geophysical Research Letters*, *42*(8), 2836–2843. https://doi.org/10.1002/2015GL063044

Covington, M. D., & Vaughn, K. A. (2019). Carbon dioxide and dissolution rate dynamics within a karst underflow-overflow system, Savoy Experimental Watershed, Arkansas, USA. *Chemical Geology*, *527*(May 2017), 118689. https://doi.org/10.1016/j.chemgeo.2018.03.009

Croissant, T., Lague, D., Steer, P., & Davy, P. (2017). Rapid post-seismic landslide evacuation boosted by dynamic river width. *Nature Geoscience*, *10*(9), 680–684. https://doi.org/10.1038/ngeo3005

Devecchio, D. E., Heermance, R. V., Fuchs, M., & Owen, L. A. (2012). Climate-controlled landscape evolution in the western transverse ranges, California: Insights from quaternary geochronology of the Saugus formation and strath terrace flights. *Lithosphere*, *4*(2), 110–130. https://doi.org/10.1130/L176.1

DiBiase, R. A., Rossi, M. W., & Neely, A. B. (2018). Fracture density and grain size controls on the relief structure of bedrock landscapes. *Geology*, *46*(5), 399–402. https://doi.org/10.1130/G40006.1

Dühnforth, M., Anderson, R. S., Ward, D. J., & Blum, A. (2012). Unsteady late Pleistocene incision of streams bounding the Colorado Front Range from measurements of meteoric and in situ 10 Be. *Journal of Geophysical Research*, *117*(F1), 1–20. https://doi.org/10.1029/2011JF002232

Gabet, E. J. (2020). Lithological and structural controls on river profiles and networks in the northern Sierra Nevada (California, USA). *Geological Society of America Bulletin*, *132*(3–4), 655–667. https://doi.org/10.1130/B35128.1

Gilbert, G. K. (1877). *Report on the geology of the Henry Mountains*. Government Printing Office.

Goodfellow, B. W., Hilley, G. E., Webb, S. M., Leonard, S. S., Moon, S., & Olson, C. A. (2016). The chemical, mechanical, and hydrological evolution of weathering granitoid. *Journal of Geophysical Research: Earth Surface*, *121*(8), 1410–1435. https://doi.org/10.1002/2016JF003822

Goudie, A. S. (2006). The Schmidt Hammer in geomorphologial research. *Progress in Physical Geography*, *30*(6), 703–718. https://doi.org/10.1177/0309133306071954

Hancock, G. S., & Anderson, R. S. (2002). Numerical modeling of fluvial strath-terrace formation in response to oscillating climate. *Geological Society of America Bulletin*, *114*(9), 1131–1142. https://doi.org/10.1130/0016-7606(2002)114<1131:NMOFST>2.0.CO;2

Hanson, P. R., Mason, J. A., & Goble, R. J. (2006). Fluvial terrace formation along Wyoming's Laramie Range as a response to increased late Pleistocene flood magnitudes. *Geomorphology*, *76*(1–2), 12–25. https://doi.org/10.1016/j.geomorph.2005.08.010

Hudson, M. R., & Murray, K. E. (2003). *Geologic map of the Ponca quadrangle, Newton, Boone, and Carroll Counties, Arkansas*. US Geological Survey Miscellaneous Field Studies Map MF–2412. 1:2400 scale.

Hudson, M. R., & Turner, K. J. (2007). *Geologic map of the boxley quadrangle, Newton and Madison Counties, Arkansas*. Geologic Map of the Boxley Quadrangle, Newton and Madison Counties, Arkansas. US Geological Survey Scientific Investigations Map 2991. 1:24,000 scale.

Johnson, K. N., & Finnegan, N. J. (2015). A lithologic control on active meandering in bedrock channels. *Bulletin of the Geological Society of America*, *127*(11–12), 1766–1776. https://doi.org/10.1130/B31184.1

Keen-Zebert, A., Hudson, M. R., Shepherd, S. L., & Thaler, E. A. (2017). The effect of lithology on valley width, terrace distribution, and bedload provenance in a tectonically stable catchment with flat-lying stratigraphy. *Earth Surface Processes and Landforms*, *42*(10), 1573–1587. https://doi.org/10.1002/esp.4116

Korup, O. (2008). Rock type leaves topographic signature in landslide-dominated mountain ranges. *Geophysical Research Letters*, *35*(11), 1–5. https://doi.org/10.1029/2008GL034157

Langston, A. L., Groeber, O. H., & Robertson, C. H. (2024). BuffaloTalusData. [Dataset]. https://doi.org/10.5281/zenodo.10463303

Langston, A. L., & Robertson, C. H. (2023). Wide bedrock valley development and sensitivity to environmental perturbations: Insights from flume experiments in erodible bedrock. *Earth Surface Processes and Landforms*, *48*(15), 1–18. https://doi.org/10.1002/esp.5680

Langston, A. L., & Temme, A. J. A. M. (2019). Impacts of lithologically controlled mechanisms on downstream bedrock valley widening. *Geophysical Research Letters*, *46*(21), 12056–12064. https://doi.org/10.1029/2019GL085164

Langston, A. L., & Tucker, G. E. (2018). Developing and exploring a theory for the lateral erosion of bedrock channels for use in landscape evolution models. *Earth Surface Dynamics*, *6*(1), 1–27. https://doi.org/10.5194/esurf-6-1-2018

Larimer, J. E., Yanites, B. J., & Jung, S. J. (2022). A field study on the lithological influence on the interaction between weathering and abrasion processes in bedrock rivers. *Journal of Geophysical Research: Earth Surface*, *127*(4), 1–17. https://doi.org/10.1029/2021JF006418

Limaye, A., & Lamb, M. P. (2014). Numerical simulations of bedrock valley evolution by meandering rivers with variable bank material. *Journal of Geophysical Research: Earth Surface*, *119*(4), 927–950. https://doi.org/10.1002/2013JF002997

MacKenzie, L. G., & Eaton, B. C. (2017). Large grains matter: Contrasting bed stability and morphodynamics during two nearly identical experiments. *Earth Surface Processes and Landforms*, *42*(8), 1287–1295. https://doi.org/10.1002/esp.4122

MacKenzie, L. G., Eaton, B. C., & Church, M. (2018). Breaking from the average: Why large grains matter in gravel-bed streams. *Earth Surface Processes and Landforms*, *43*(15), 3190–3196. https://doi.org/10.1002/esp.4465

Malatesta, L. C., Prancevic, J. P., & Avouac, J. P. (2017). Autogenic entrenchment patterns and terraces due to coupling with lateral erosion in incising alluvial channels. *Journal of Geophysical Research: Earth Surface*, *122*(1), 335–355. https://doi.org/10.1002/2015JF003797

May, C., Roering, J., Eaton, L. S., & Burnett, K. M. (2013). Controls on valley width in mountainous landscapes: The role of landsliding and implications for salmonid habitat. *Geology*, *41*(4), 503–506. https://doi.org/10.1130/G33979.1

Merritts, D. J., Vincent, K. R., & Wohl, E. E. (1994). Long river profiles, tectonism, and eustasy: A guide for interpreting fluvial terraces. *Journal of Geophysical Research*, *99*(B7), 14031–14050. https://doi.org/10.1029/94JB00857

Meyer, G. A., Wells, S. G., & Jull, A. J. T. (1995). Fire and alluvial chronology in yellowstone national park: Climatic and intrinsic controls on holocene geomorphic processes. *Geological Society of America Bulletin*, *107*(10), 1211–1230. https://doi.org/10.1130/0016-7606(1995)107<1211:FAACIY>2.3.CO;2

Montgomery, D. R. (2001). Slope distributions, threshold hillslopes, and steady-state topography. *American Journal of Science*, *301*(4–5), 432–454. https://doi.org/10.2475/ajs.301.4-5.432

Montgomery, D. R. (2004). Observations on the role of lithology in strath terrace formation and bedrock channel width. *American Journal of Science*, *304*(5), 454–476. https://doi.org/10.2475/ajs.304.5.454

Murphy, B. P., Johnson, J. P. L., Gasparini, N. M., & Sklar, L. S. (2016). Chemical weathering as a mechanism for the climatic control of bedrock river incision. *Nature*, *532*(7598), 223–227. https://doi.org/10.1038/nature17449

Neely, B. L. (1985). *The flood of December 1982 and the 100- and 500-year flood on the Buffalo River, Arkansas*. U.S. Geological Survey Water-Resources Investigations Report 85-4192. https://doi.org/10.3133/wri854192

Pan, B., Burbank, D., Wang, Y., Wu, G., Li, J., & Guan, Q. (2003). A 900 k.y. record of strath terrace formation during glacial-interglacial transitions in northwest China. *Geology*, *31*(11), 957–960. https://doi.org/10.1130/G19685.1

Parker, G. (1978). Self-formed straight rivers with equilibrium banks and mobile bed. Part 2. The gravel river. *Journal of Fluid Mechanics*, *89*(1), 127–146. https://doi.org/10.1017/S0022112078002505

Roda-Boluda, D. C., D'Arcy, M., McDonald, J., & Whittaker, A. C. (2018). Lithological controls on hillslope sediment supply: Insights from landslide activity and grain size distributions. *Earth Surface Processes and Landforms*, *43*(5), 956–977. https://doi.org/10.1002/esp.4281

Schanz, S. A., & Montgomery, D. R. (2016). Lithologic controls on valley width and strath terrace formation. *Geomorphology*, *258*, 58–68. https://doi.org/10.1016/j.geomorph.2016.01.015

Schanz, S. A., Montgomery, D. R., Collins, B. D., & Duvall, A. R. (2018). Multiple paths to straths: A review and reassessment of terrace genesis. *Geomorphology*, *312*, 12–23. https://doi.org/10.1016/j.geomorph.2018.03.028

Schmidt, K. M., & Montgomery, D. R. (1995). Limits to relief. *Science*, *270*(5236), 617–620. https://doi.org/10.1126/science.270.5236.617

Scott, D. N., & Wohl, E. E. (2019). Bedrock fracture influences on geomorphic process and form across process domains and scales. *Earth Surface Processes and Landforms*, *44*(1), 27–45. https://doi.org/10.1002/esp.4473

Shobe, C. M., Turowski, J. M., Nativ, R., Glade, R. C., Bennett, G. L., & Dini, B. (2021). The role of infrequently mobile boulders in modulating landscape evolution and geomorphic hazards. *Earth-Science Reviews*, *220*(January), 103717. https://doi.org/10.1016/j.earscirev.2021.103717

Sklar, L. S., Riebe, C. S., Marshall, J. A., Genetti, J., Leclere, S., Lukens, C. L., & Merces, V. (2017). The problem of predicting the size distribution of sediment supplied by hillslopes to rivers. *Geomorphology*, *277*, 31–49. https://doi.org/10.1016/j.geomorph.2016.05.005

Snyder, N. P., Whipple, K. X., Tucker, G. E., & Merritts, D. J. (2003). Channel response to tectonic forcing: Field analysis of stream morphology and hydrology in the Mendocino triple junction region, northern California. *Geomorphology*, *53*(1), 97–127. https://doi.org/10.1016/s0169-555x(02)00349-5

Spotila, J. A., Moskey, K. A., & Prince, P. S. (2015). Geologic controls on bedrock channel width in large, slowly-eroding catchments: Case study of the New River in eastern North America. *Geomorphology*, *230*, 51–63. https://doi.org/10.1016/j.geomorph.2014.11.004

Thaler, E. A., & Covington, M. D. (2016). The influence of sandstone caprock material on bedrock channel steepness within a tectonically passive setting: Buffalo National River Basin, Arkansas, USA. *Journal of Geophysical Research: Earth Surface*, *121*(9), 1635–1650. https://doi.org/10.1002/2015JF003771

Tofelde, S., Bufe, A., & Turowski, J. M. (2022). Hillslope sediment supply limits alluvial valley width. *AGU Advances*, *3*(6). https://doi.org/10.1029/2021AV000641

Tomkin, J. H., Brandon, M. T., Pazzaglia, F. J., Barbour, J. R., & Willett, S. D. (2003). Quantitative testing of bedrock incision models for the Clearwater River, NW Washington State. *Journal of Geophysical Research*, *108*(B6). https://doi.org/10.1029/2001jb000862

Turowski, J. M., Bufe, A., & Tofelde, S. (2023). A process-based model for fluvial valley width. *EGUsphere*, *2023*, 1–38. https://doi.org/10.5194/egusphere-2023-1770

U.S. Geological Survey. (2023). 3D elevation program 9-meter resolution digital elevation model. [Dataset]. Retrieved from https://apps.nationalmap.gov/downloader/

Vandenberghe, J. (2003). Climate forcing of fluvial system development: An evolution of ideas. *Quaternary Science Reviews*, *22*(20), 2053–2060. https://doi.org/10.1016/S0277-3791(03)00213-0

Verdian, J. P., Sklar, L. S., Riebe, C. S., & Moore, J. R. (2020). Sediment size on talus slopes correlates with fracture spacing on bedrock cliffs: Implications for predicting initial sediment size distributions on hillslopes. *Earth Surface Dynamics*, *9*(4), 1073–1090. https://doi.org/10.5194/esurf-9-1073-2021

Wegmann, K. W., & Pazzaglia, F. J. (2002). Holocene strath terraces, climate change, and active tectonics: The Clearwater River basin, Olympic Peninsula, Washington State. *Bulletin of the Geological Society of America*, *114*(6), 731–744. https://doi.org/10.1130/0016-7606(2002)114<0731:HSTCCA>2.0.CO;2

Whipple, K. X. (2004). Bedrock rivers and the geomorphology of active Orogens. *Annual Review of Earth and Planetary Sciences*, *32*(1), 151–185. https://doi.org/10.1146/annurev.earth.32.101802.120356

Whittaker, A. C. (2012). How do landscapes record tectonics and climate? *Lithosphere*, *4*(2), 160–164. https://doi.org/10.1130/RF.L003.1

Wilcock, P. R., & McArdell, B. W. (1993). Surface-based fractional transprot rates: Partial transport and mobilization thresholds. *Water Resources Research*, *29*(4), 1297–1312. https://doi.org/10.1029/92wr02748

Wobus, C., Whipple, K. X., Kirby, E., Snyder, N., Johnson, J., Spyropolou, K., et al. (2006). Tectonics from topography: Procedures, promise, and pitfalls. *Special Papers - Geological Society of America*, *398*(September 2016), 55–74. https://doi.org/10.1130/2006.2398(04

Wohl, E. (2008). The effect of bedrock jointing on the formation of straths in the Cache la Poudre River drainage. *Colorado Front Range*, *113*(Table 1), 1–12. https://doi.org/10.1029/2007JF000817

Wohl, E., & David, G. C. L. (2008). Consistency of scaling relations among bedrock and alluvial channels. *Journal of Geophysical Research*, *113*(4), 1–16. https://doi.org/10.1029/2008JF000989

Yager, E. M., & Schmeeckle, M. W. (2013). The influence of vegetation on turbulence and bed load transport. *Journal of Geophysical Research: Earth Surface*, *118*(3), 1585–1601. https://doi.org/10.1002/jgrf.20085

Yager, E. M., Schmeeckle, M. W., & Badoux, A. (2018). Resistance is not Futile: Grain resistance controls on observed critical shields stress variations. *Journal of Geophysical Research: Earth Surface*, *123*(12), 3308–3322. https://doi.org/10.1029/2018JF004817

Yang, J. Q., Kerger, F., & Nepf, H. M. (2015). Estimation of the bed shear stress in vegetated and bare channels with smooth beds. *Water Resources Research*, *51*(5), 3647–3663. https://doi.org/10.1002/2014WR016042

Zunka, J. P. P. (2018). *Controls on process and form in alluvial and bedrock meandering rivers*. PhD Dissertation (p. 155). Oregon State University.